

Role of Deprotonation Events in Ubihydroquinone:Cytochrome *c* Oxidoreductase from Bovine Heart and Yeast Mitochondria

Ulrich Brandt* and Jürgen G. Okun

Zentrum der Biologischen Chemie, Universitätsklinikum Frankfurt, D-60590 Frankfurt am Main, Federal Republic of Germany

Received April 24, 1997; Revised Manuscript Received July 7, 1997[®]

ABSTRACT: The pH dependence of bovine and yeast cytochrome *bc*₁ complex catalyzing electron transfer from ubi- and plastoquinone to cytochrome *c* have been analyzed. The pH dependence of the steady-state rate was found to be governed by two protonable groups, one of which ($pK \approx 6.6$) has to be deprotonated while the other ($pK \approx 9.2$) has to be protonated to allow catalysis. Using ubiquinol instead of ubiquinone as a substrate resulted in 1.4- and 1.7-fold lower steady-state rates for the bovine and yeast enzymes, respectively. The activation energy at pH 8.0 was 33 kJ/mol for the bovine and 44 kJ/mol for the yeast enzyme and exhibited a linear decrease between pH 5.4 and 9.2. For ubiquinol the slope was very close to a value of -5.7 kJ/mol expected if the activation energy depended on a single deprotonation event. When plastoquinone was used instead, the slope more than doubled, indicating that a second deprotonation contributed to the activation barrier with this nonphysiological substrate. In contrast to previous kinetic models for the cytochrome *bc*₁ complex, which propose that the activation barrier is associated with the formation of ubisemiquinone at the ubiquinol oxidation center, our results strongly suggest that the best approximation of the transition state is the singly deprotonated form of ubiquinol. This supports the recently proposed proton-gated charge transfer mechanism, which has control of catalysis by the first deprotonation of ubiquinol as one of its key features [Brandt, U. (1996) *FEBS Lett.* 387, 1–6]. All results reported here can be rationalized in a straightforward way based on other aspects of the same hypothesis.

The proton-pumping ubiquinol:cytochrome *c* oxidoreductase (cytochrome *bc*₁ complex) forms the middle part of the mitochondrial and bacterial respiratory chains. It catalyzes the electron transfer from ubiquinol to cytochrome *c* and links this reaction to the translocation of protons across the inner mitochondrial membrane or bacterial plasma membrane.

The generally accepted mechanistic concept for the protonmotive electron transfers within the cytochrome *bc*₁ complex is the Q-cycle reaction scheme introduced by Peter Mitchell (Mitchell, 1975). At center P¹ (Q_o) of the Q-cycle, the two electrons resulting from ubiquinol oxidation follow divergent pathways in a strictly coupled fashion (Brandt & Trumpower, 1994). This bifurcation is essential for the protonmotive action of the cytochrome *bc*₁ complex, as it links the reduction of the rather positive Rieske iron–sulfur cluster ($E_{m7} = +290$ mV) to the reduction of the ≈ 300 mV more negative heme *b*_L. The electron transferred to heme *b*_L is used to eventually rereduce ubiquinone at center N (Q_i).

From single-turnover experiments with bacterial chromatophores, a rate constant of 1700 s^{-1} and an activation barrier of 32 kJ/mol at pH 7 have been deduced for the oxidation of ubiquinol at center P (Crofts & Wang, 1989). It has been suggested that this activation barrier reflects the formation of a highly unstable semiquinone at center P during catalysis, and kinetic models of the Q-cycle were based on this assumption (Ding et al., 1995; Crofts & Wang, 1989). However, there is no experimental evidence that a highly unstable semiquinone, which has been observed only under very specific experimental conditions (de Vries et al., 1981), is formed during normal catalysis. In fact, assigning the activation barrier to the semiquinone does not account for the first deprotonation step of ubiquinol (Brandt, 1996), which has to precede the first electron transfer and titrates with a pK of 11.3 in 80% ethanol (Rich, 1984). Remarkably, the energetic consequences associated with this initial deprotonation have not been investigated so far.

The recently published proton-gated charge transfer model for the mechanism of center P (Brandt, 1996) postulates that the first deprotonation of ubiquinol controls catalysis by promoting the symproportionation of a charge transfer complex formed by two ubiquinone molecules that have been reported to be bound at center P (Ding et al., 1992).

To test this hypothesis and to address the question which role protonation and deprotonation events play within the reaction cycle of the cytochrome *bc*₁ complex, we have studied the pH dependence and the isotope effect for the steady-state reaction of the mitochondrial enzyme. The study was performed with cytochrome *bc*₁ complex from two different sources, bovine heart and *Saccharomyces cerevisiae*, to identify possible species-specific properties. To rule

* To whom correspondence should be addressed at Zentrum der Biologischen Chemie, Universitätsklinikum Frankfurt, Theodor-Stern-Kai 7, Haus 25B, 60590 Frankfurt am Main, Germany. Tel. +49 69 6301 6926; Fax +49 69 6301 6970; E-mail brandt@zbc.klinik.uni-frankfurt.de.

[®] Abstract published in *Advance ACS Abstracts*, September 1, 1997.

¹ Abbreviations: BSA, bovine serum albumin; E_a , macroscopic activation energy; center P and N, ubiquinone reaction centers on the positive and negative side of the mitochondrial membrane; Mes, 2-(*N*-morpholino)ethanesulfonic acid; Mops, 3-(*N*-morpholino)propanesulfonic acid; NBH, *n*-nonylubi-*n*-hydroquinone; NBD, *n*-nonylubi-*n*-dehydroquinone; PBH, *n*-decylplastoquinone; Taps, *N*-[tris(hydroxymethyl)methyl]-3-aminopropanesulfonic acid.

out possible artifacts due to the hydrophobic nature of the ubiquinone interacting with a large membrane protein complex, we compared data obtained with detergent-solubilized cytochrome *bc*₁ complex and with enzyme reconstituted into proteoliposomes.

EXPERIMENTAL PROCEDURES

Isolation of Mitochondrial Cytochrome *bc*₁ Complex. Bovine heart cytochrome *bc*₁ complex was prepared as described by Schagger et al. (1986). Yeast cytochrome *bc*₁ complex was purified from *S. cerevisiae* KM91 using the method of Geier et al. (1992). In both protocols, chromatography on Sepharose CL-6B equilibrated with 0.05% Triton X-100, 100 mM NaCl, 2 mM NaN₃, and 20 mM Na⁺/Mops, pH 7.2, was the final step. Fractions containing cytochrome *bc*₁ complex were collected and concentrated to around 40 μ M cytochrome *b* by ultrafiltration through a YM-100 membrane (Amicon).

Preparation of Proteoliposomes. Unilamellar proteoliposomes were prepared by cholate dialysis (Kagawa & Racker, 1971) with egg yolk phospholipid as described earlier (Brandt et al., 1988). The protein to phospholipid ratio was 1:10 000 (mol/mol) and the orientation of the incorporated complexes was more than 95% right side out as determined by the ascorbate reduction method described earlier (Brandt et al., 1988).

Substrates. Nonylubiquinone was prepared essentially following the protocol of Wan et al. (1975). Decylplastoquinone was obtained from Sigma. The quinones were reduced to nonylubihydroquinone (NBH), decylplastohydroquinone (PBH), and nonylubideuteroquinone (NBD) as follows: 40–60 mg of the quinone was dissolved in 3 mL of hexane (ubiquinone) or diethyl ether (plastoquinone) in a tight vessel kept under argon or nitrogen. After 3 mL of water or D₂O was added (to make NBD), dithionite was added until the hexane phase was colorless. After removal of the aqueous phase, the organic phase was washed twice with 0.5 M NaCl to remove excess dithionite. The solvent was evaporated and the product was dissolved in dimethyl sulfoxide containing 1 mM HCl. The reduced quinones were stored at –20 °C in small portions under argon or nitrogen. The identity of the ubiquinone derivatives and the replacement of the hydroxyl protons by deuterons in the case of NBD was verified by ¹H nuclear magnetic resonance spectroscopy. Hydroquinone concentrations were determined spectrophotometrically at 290 nm ($\epsilon = 4.2 \text{ mM}^{-1} \text{ cm}^{-1}$).

Measurements of Steady-State Kinetics. Steady-state activity of cytochrome *bc*₁ complex was recorded as the rate of cytochrome *c* reduction in a Perkin-Elmer 156 dual-wavelength spectrophotometer at 550–540 nm ($\epsilon = 19 \text{ mM}^{-1} \text{ cm}^{-1}$) using a stirred and thermostated cuvette with a final volume of 2 mL. Buffer was 50 mM KCl, 2 mM NaN₃, and 0.2 mM EDTA, buffered with 50 mM K⁺/Mes (pH 5.4–6.6), K⁺/Mops (pH 6.8–7.8), or K⁺/Taps (pH 8.0–9.2). Bovine serum albumin (BSA, 0.1%) was added to prevent rapid precipitation of the quinone, if detergent-solubilized enzyme was used. Cytochrome *bc*₁ complex proteoliposomes, for which the term reconstituted enzyme will be used in the following, were diluted to 0.5 μ M and uncoupled by preincubation with 2 μ M carbonyl cyanide *p*-(trifluoromethoxy)phenylhydrazine and 1 μ M valinomycin.

After addition of 50 μ M horse heart cytochrome *c*, the reduced quinone was added. Then the reaction was started

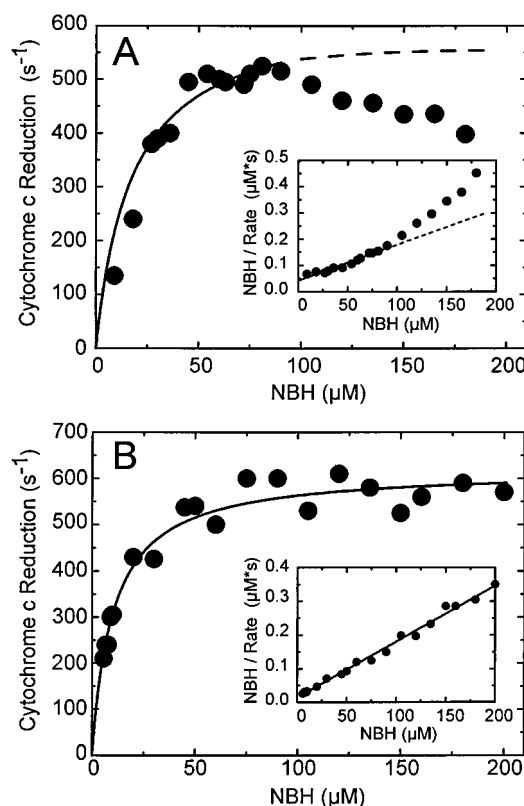


FIGURE 1: Michaelis–Menten Kinetics of Cytochrome *bc*₁ Complex. The steady-state rate of cytochrome *c* reduction at pH 7.2 was measured with cytochrome *bc*₁ complex from bovine heart solubilized in detergent in the presence of 0.1% BSA (A) and reconstituted into proteoliposomes (B) as described in Experimental Procedures. Data collected at 25 °C were fitted using the standard Michaelis–Menten equation. In panel A only the data in the range of the solid line were used for numerical analysis, and the dashed line represents an extrapolation over the whole concentration range of the experiment. The insets show a linearized representation according to Hanes. The fitted K_M values were 13 μ M (A) and 10 μ M (B), and the fitted maximal turnover numbers were 610 s⁻¹ (A) and 620 s⁻¹ (B).

by the addition of 2.5 nM cytochrome *bc*₁ complex. The slopes were corrected for the noncatalytic rate of cytochrome *c* reduction by the hydroquinone observed prior to the addition of enzyme, which increases with pH and makes reliable measurements above pH 9.2 impossible.

Data were analyzed using the PsipLOT software package version 4.61 (Poly Software International). The numerical procedure used to fit experimental data was the Marquardt algorithm (Marquardt, 1963).

RESULTS

Validation of the Steady-State Assay. The rate constants for the individual electron transfer reactions of the cytochrome *bc*₁ complex suggest that in the presence of saturating substrate concentrations the overall rate is governed by the oxidation of ubihydroquinone at center P (Crofts & Wang, 1989). However, due to the complexity of the enzyme under investigation and the amphipathic nature of one of the substrates, special caution has to be used to choose appropriate experimental conditions for steady-state analysis. Figure 1 shows the dependence of the rate of cytochrome *c* reduction on the concentration of ubihydroquinone. With detergent-solubilized cytochrome *bc*₁ complex from bovine heart (Figure 1A), the rate increase followed Michaelis–Menten

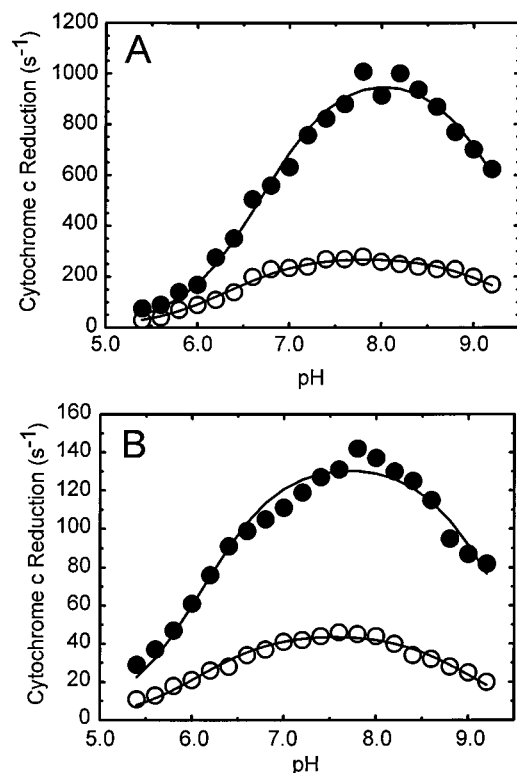


FIGURE 2: pH Dependence of Activity. The steady-state rates of cytochrome *c* reduction by reconstituted cytochrome *bc*₁ complex over a pH range from 5.4 to 9.2 at saturating substrate concentrations were measured as described in Experimental Procedures. The lines represent the least-squares fit of the data obtained at 24 °C using eq 1 given in the Results section. The fitted parameters are given in Table 1. (A) NBH; (B) PBH. (●) Bovine enzyme; (○) yeast enzyme.

behavior up to about 80 μ M NBH. Above this substrate concentration a decrease of the catalytic rate was observed. This is explained by formation of ubihydroquinone micelles, which is expected to lower the effective concentration of substrate available for the enzymatic reaction. This effect was not observed with cytochrome *bc*₁ complex reconstituted into liposomes (Figure 1B). Obviously, partitioning of NBH into the liposomal membrane prevented micelle formation and strict Michaelis–Menten behavior was observed over the entire concentration range tested.

Very similar behavior was observed with yeast cytochrome *bc*₁ complex or when PBH was used as a substrate (data not shown). These results were used to empirically choose ubihydroquinone concentrations at which the rate approached its maximum and micelle formation was minimal. Following this analysis, hydroquinones were used at 75 μ M for bovine enzyme and 120 μ M for yeast enzyme to reach quasi-saturating conditions. With both organisms a K_m for cytochrome *c* of about 6 μ M was observed (data not shown) and a concentration of 50 μ M for this substrate was used in all tests.

pH Dependence of Cytochrome *c* Reductase Activity. For both bovine and yeast enzyme the pH profile for the cytochrome *c* reductase assay was a bell-shaped curve with a maximum between pH 7.5 and 8.0 with NBH and PBH (Figure 2). Over the tested pH range from 5.4 to 9.2 the rates observed for yeast enzyme were about a third for both substrates when compared to bovine enzyme. However, depending on the batch of enzyme used this ratio varied between 1.5 and 4. The rates obtained with NBH (Figure

Table 1: p*K* Values Controlling Steady-State Activity^a

	NBH		PBH	
	p <i>K</i> _A	p <i>K</i> _B	p <i>K</i> _A	p <i>K</i> _B
bovine				
solubilized enzyme	6.7 ± 0.1	9.1 ± 0.1	nd	nd
reconstituted enzyme	6.7 ± 0.1	9.3 ± 0.1	6.1 ± 0.1	9.3 ± 0.1
yeast				
solubilized enzyme	6.5 ± 0.1	9.1 ± 0.1	nd	nd
reconstituted enzyme	6.3 ± 0.1	9.4 ± 0.1	6.1 ± 0.1	9.0 ± 0.1

^a The p*K* values for 24 °C were fitted using eq 1 given in the Results section. See legend of Figure 2 for experimental conditions and text for further details.

2A) were about 6–7 times higher than those with PBH (Figure 2B) for both enzymes.

In all cases the pH dependence of steady-state activity could be simulated quite well (Figure 2) by

$$v = V_{\text{opt}} \frac{1}{1 + \frac{[\text{H}^+]}{K_A}} \frac{1}{1 + \frac{K_B}{[\text{H}^+]}} \quad (1)$$

where v is the observed rate, $[\text{H}^+]$ is the concentration of protons, K_A and K_B are the dissociation constants of two protonable groups A and B, and V_{opt} is the optimal catalytic rate that would be observed if group A was deprotonated and group B was protonated in all enzyme molecules.

Table 1 summarizes the p*K* values that were determined by fitting the experimental data given in Figure 2 to eq 1. p*K*_A was between 6.3 and 6.7 when NBH was used and 6.1 when PBH was used. p*K*_B was between 9.1 and 9.4 with both substrates. No significant difference was observed between cytochrome *bc*₁ complexes from the two different organisms and the two forms in which the enzyme was added.

It was not possible to improve the simulation of the experimental data by assuming additional protonable groups or by taking into account that the midpoint potential of the Rieske iron–sulfur cluster drops off markedly above pH 7 (Prince & Dutton, 1976; Kuila & Fee, 1986; Link et al., 1992). We conclude that the observed pH dependence of the steady-state activity was largely determined by the population of cytochrome *bc*₁ complexes in which group A was deprotonated and group B was protonated.

Activation Barrier and Isotope Effect. The activation barrier (E_a) of the steady-state reaction was determined from the temperature dependence of the cytochrome *c* reduction rate between 14 and 32 °C (Table 2). Figure 3 shows Arrhenius plots obtained with bovine and yeast enzyme at pH 8.0. At 33 ± 2 kJ/mol the activation barrier for bovine cytochrome *bc*₁ complex was significantly lower than the 44 ± 3 kJ/mol found for the yeast enzyme. When measurements were made in buffer made with D₂O and the substrate was the deuterioquinone instead of the hydroquinone, no significant effect on E_a was found but the rates of cytochrome *c* reduction were significantly lower (Figure 3). This kinetic isotope effect resulted in a decrease of the observed rate by a factor of 1.4 ± 0.1 for the bovine and 1.7 ± 0.2 for the yeast enzyme.

pH Dependence of the Activation Barrier. The activation barrier (E_a) was found to be inversely proportional to pH over the entire range tested. With NBH and reconstituted

Table 2: Activation Barrier: Isotope Effect and pH Dependence^a

	E_a at pH 8		NBH		PBH	
	NBH	NBD	E_a^0 (kJ·mol ⁻¹)	slope (kJ·mol ⁻¹ ·pH ⁻¹)	E_a^0 (kJ·mol ⁻¹)	slope (kJ·mol ⁻¹ ·pH ⁻¹)
bovine						
solubilized enzyme	33 ± 2	38 ± 2	78 ± 3	-5.6 ± 0.4	nd	nd
reconstituted enzyme	34 ± 2	nd	77 ± 2	-5.4 ± 0.3	145 ± 4	-14.1 ± 0.5
yeast						
solubilized enzyme	44 ± 3	43 ± 4	94 ± 4	-6.3 ± 0.6	nd	nd
reconstituted enzyme	44 ± 2	nd	91 ± 3	-5.9 ± 0.4	150 ± 8	-12.6 ± 1.1

^a Activation energies were obtained from Arrhenius plots as described in legends of Figures 3 and 4. Standard deviations were derived from linear regression analysis. See text for further details.

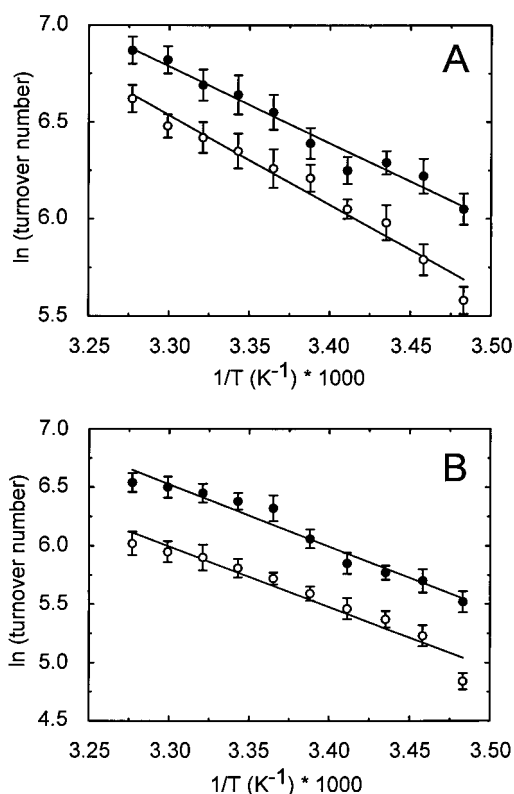


FIGURE 3: Activation Barrier and Isotope Effect. The temperature dependence of the steady-state rates of cytochrome *c* reduction by solubilized cytochrome *bc*₁ complex at pH 8.0 and saturating substrate concentration was measured between 14 and 32 °C as described in Experimental Procedures. The data were linearized by using the Arrhenius plot to determine the macroscopic activation barrier E_a . Error bars represent the standard deviation from three measurements. See text for the corresponding E_a values and for further details. (A) Bovine enzyme; (B) yeast enzyme. (●) NBH; (○) NBD (in D₂O).

enzyme (Figure 4A) the slope was -5.4 ± 0.3 kJ·mol⁻¹·pH⁻¹ for bovine and -5.9 ± 0.4 kJ·mol⁻¹·pH⁻¹ for yeast cytochrome *bc*₁ complex. Almost identical values were obtained with detergent-solubilized enzymes (Table 2). In all cases the experimental slope was close to -5.7 kJ·mol⁻¹·pH⁻¹ (dotted lines in Figure 4A), which is the theoretical value, if an $n = 1$ deprotonation event is a major component of the activation barrier. This means that the observed pH dependence of the activation barrier could be described by

$$E_a = E_a^0 + nRT \ln [H^+] = E_a^0 - 5.7n(\text{pH}) \quad (2)$$

where E_a^0 is the activation barrier extrapolated to pH = 0, n is the stoichiometry factor, R is the gas constant, T is the

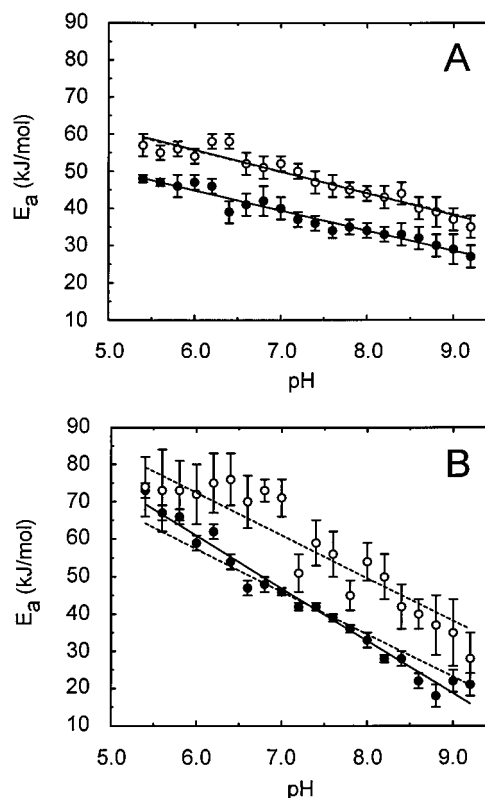


FIGURE 4: pH Dependence of Activation Barrier. Secondary plot of activation energies obtained by Arrhenius plots (see Figure 3) over a pH range of 5.4 to 9.2. Error bars represent the standard deviation calculated from linear regression analysis of the corresponding Arrhenius plots. Solid lines represent the best fit obtained by linear regression; dashed lines represent the best fit obtained by using eqs 3 and 4 for panels A and B, respectively. (A) NBH; (B) PBH. (●) bovine enzyme; (○) yeast enzyme.

absolute temperature (298 K), and $[H^+]$ is the concentration of protons.

It follows that the energy required to deprotonate a group HX should contribute to E_a^0 , according to

$$E_a^0 = -RT \ln K_{HX} + C \quad (3)$$

where C represents any pH-independent contributions to the activation barrier. By neglecting these contributions and setting $C = 0$, we could calculate limit values of $pK_{HX} \approx 14$ from the data obtained with bovine enzyme and $pK_{HX} \approx 16$ from those obtained with the yeast enzyme.

When PBH was used as a substrate (Figure 4B), the pH dependence of the activation barrier again followed a linear relationship, but the slopes for both organisms were found to be at least twice as steep as with NBH, which carries the

physiological ubiquinone headgroup (Table 2). In this case, application of eq (2) and assuming an exact $n = 2$ deprotonation stoichiometry still resulted in a reasonable description of the experimental data (dotted lines in Figure 4B). In terms of E_a^0 this suggests that for PBH eq 3 should be extended by introducing a second deprotonating group HY:

$$E_a^0 = -RT \ln K_{HX} - RT \ln K_{HY} + C \quad (4)$$

It seemed not unreasonable to assume that such a group HY was an additional feature not observed with NBH and that the same group HX was one of the deprotonating groups controlling E_a with PBH. Therefore, we could estimate limit values of $pK_{HY} \approx 11$ for the data obtained with bovine enzyme and $pK_{HY} \approx 10$ for those obtained with the yeast enzyme by using the limit values for K_{HX} estimated from the experiments with NBH and by again neglecting the contribution of C .

The simplified interpretation of E_a^0 given by eqs 3 and 4 is by no means exact and it is difficult to estimate the contribution and components of C from the macroscopic approach used here (see Discussion). However, the pH-independent contribution of C has no effect on the slope of the plot. Therefore, the data clearly indicate that formation of the transition state of the cytochrome bc_1 complex reaction involves one deprotonation step with the ubihydroquinone derivative NBH and at least two deprotonation steps with the plastoquinone derivative PBH. It is remarkable that the nonlinear decrease of the midpoint potential of the Rieske iron-sulfur cluster from +310 to +200 mV observed between pH 7 and 9 (Link et al., 1992) seemed to have no effect on the activation barrier of the steady-state reaction.

DISCUSSION

Analysis of the steady-state mode of the cytochrome bc_1 complex requires the use of hydrophobic ubiquinones at rather high concentrations. The amphipathic nature of this substrate and the use of detergents during isolation make the assay of this enzyme prone to artifacts caused by micelle formation and aggregation of the substrate or the membrane protein complex. To exclude that such problems affected our results, we compared data obtained with cytochrome bc_1 complex solubilized in detergent and reconstituted into a liposomal membrane. The fact that no significant differences were observed between these two preparations (see Tables 1 and 2) also indicated that it was not important for the observations made whether the cytochrome bc_1 complex was embedded in a membrane or not.

Additional complications could have been caused by inadvertent modifications to the multiprotein complexes during its purification. We therefore used cytochrome bc_1 complex from two different eucaryotic organisms that are known to differ in the way the Rieske iron-sulfur protein, a structural component of center P (Brandt et al., 1991; Iwata et al., 1996), is associated. While in bovine heart this subunit can be dissociated reversibly (Trumpower & Edwards, 1979; Engel et al., 1983), the yeast subunit is bound much tighter and cannot be removed without denaturing the rest of the multiprotein complex (Geier et al., 1992; Giessler et al., 1994). Comparison of these two rather distant eucaryotes also gave some idea on the variability of the measured

parameters. While one would not have expected any qualitative differences, it is remarkable that the only significant quantitative difference was the 25% higher activation barrier of the yeast enzyme.

Nature of the Protonatable Groups Controlling Steady-State Activity. The pH profiles of the steady-state activity could be modeled by equation [1], indicating that two protonatable groups with pK values near 6.6 and 9.2 were essential for turnover of the cytochrome bc_1 complex in an all-or-nothing fashion. In other words, only the population of enzymes in which the more acidic group was dissociated and the more basic group was protonated seemed to contribute to steady-state activity. For plant cytochrome bf complex a remarkably similar pH profile for the rate of cytochrome f reduction has been reported (Bendall, 1982) but was interpreted differently, assuming that the first electron transfer was the rate-limiting step. However, in particular at higher pH values, this interpretation allowed only a rather poor simulation of the experimental data. For bovine heart cytochrome bc_1 complex a pH profile has been reported earlier but could only be fitted up to pH 8.5 using only a single pK value (Link & von Jagow, 1995), which was identical to the lower pK found in the present study.

A protonatable group with a pK value around 6.6 has not been found to be associated with any of the redox prosthetic groups of the cytochrome bc_1 complex. A straightforward interpretation would be that this group is the primary acceptor group of a proton pathway leading from hydroquinone to the bulk phase at center P.

A pK value of 9.2 has been reported for the second redox Bohr group associated with the Rieske iron-sulfur cluster (Link et al., 1992). On the basis of evidence from circular dichroism spectroscopy, it has been proposed that these redox-Bohr groups are the two histidines coordinating the iron-sulfur center (Link, 1994). It has also been suggested from different lines of evidence that these histidines might be directly involved in binding ubiquinone at center P (Ding et al., 1992; Link, 1994; Kraiczky et al., 1996). This notion was supported recently by the high-resolution structure of a water-soluble fragment of the Rieske iron-sulfur protein, which shows that these residues form a tip of this subunit (Iwata et al., 1996). Therefore, it seems very likely that the group with a pK value of 9.2 which has to be protonated in active cytochrome bc_1 complex is one of the histidines coordinating the iron-sulfur cluster. A hydrogen bond between one of these histidines and ubiquinone also plays a central role in the recently proposed proton-gated charge transfer mechanism for center P (Brandt, 1996).

On the other hand, we could find no indications for an effect of the protonation state of the other histidine ($pK_{ox} = 7.6$) on steady-state activity. Most notably, the iron-sulfur cluster, which is the primary electron acceptor at center P, increases its midpoint potential upon deprotonation of this group above pH 7.0 (Prince & Dutton, 1976; Kuila & Fee, 1986; Link et al., 1992), but a corresponding rate decrease was not observed.

Nature of the Transition State. The linear $n = 1$ pH dependence of the activation barrier and the observed isotope effect clearly indicate that a deprotonation event is involved in controlling the steady-state reaction of the mitochondrial cytochrome bc_1 complex. While it is generally acknowledged that for thermodynamic reasons a deprotonation step has to precede oxidation of ubihydroquinone (Bendall, 1982;

Rich, 1984), this step has not been discussed as a contribution to the activation barrier so far. Instead, kinetic models that have been developed for this redox enzyme (Crofts & Wang, 1989; Ding et al., 1992) propose that the activation barrier is associated with the oxidation of ubihydroquinone by the Rieske iron–sulfur cluster. In these models, the transition state has been described as a highly unstable semiquinone formed during ubihydroquinone oxidation within the overall reaction scheme of the protonmotive Q-cycle. While there is no experimental evidence for the formation of such an intermediate during normal catalysis [a semiquinone at center P is only observed in the antimycin-inhibited state (de Vries et al., 1981)], the strict pH dependence of the activation barrier reported here is difficult to reconcile with this possibility. Moreover, if formation of the transition state would be linked to the first oxidation step of the ubihydroquinone, one would expect that the activation barrier followed the highly pH-dependent midpoint potential of the iron–sulfur cluster (Prince & Dutton, 1976; Kuila & Fee, 1986; Link et al., 1992). However, this was not observed in the experiments reported here.

On the other hand, it is one of the prerequisites of the recently proposed proton-gated charge transfer mechanism (Brandt, 1996) that the center P reaction is controlled by the deprotonation of ubihydroquinone. Therefore, our results provide experimental evidence for one of the key predictions of this hypothetical mechanism.

It is much more difficult to interpret the observed linear pH dependence of the activation barrier quantitatively, in particular as the non-pH-dependent contribution (*C* in eqs 3 and 4) cannot be determined by the approach used in this study.

A very similar approach has been used by Warshel (1979) to calculate the energetic barriers associated with the protonable groups involved in the proton pump of bacteriorhodopsin. According to this work the pH-independent contributions associated with the deprotonation of these groups reflect (i) the difference in the solvation energy between aqueous solution and protein environment and (ii) a term describing the repulsion between adjacent charged species. In other words, the contribution of *C* is expected to be near zero if the electrostatic stabilization of the charged ubiquinone species is similar in the protein and the surrounding medium. It has been calculated, on the basis of the high-resolution structure of the bacterial reaction center (Lancaster et al., 1996), that the effect of a charge on a bound quinone on the electrostatic potential of the surrounding protein can vary considerably. Such detailed structural information is not yet available for the cytochrome *bc*₁ complex, but there are several arguments that the electrostatic behavior of the environment of ubiquinone bound at center P can be expected to be rather similar to the solvent and that therefore the contribution of *C* should be rather small. If the binding pocket at center P is made accessible to the surrounding medium by removing the iron–sulfur protein (Brandt et al., 1991), this has virtually no effect on the affinity and the fluorescence quenching of a bound *E*-β-methoxyacrylate inhibitor, suggesting that the dipole moment of the intact center P pocket is very similar to that of the bulk phase. Also, the significant but relatively small isotope effect can be taken as an indication that the proton movement is not associated with a pronounced reorganization barrier. Moreover, as discussed recently in detail (Brandt, 1996),

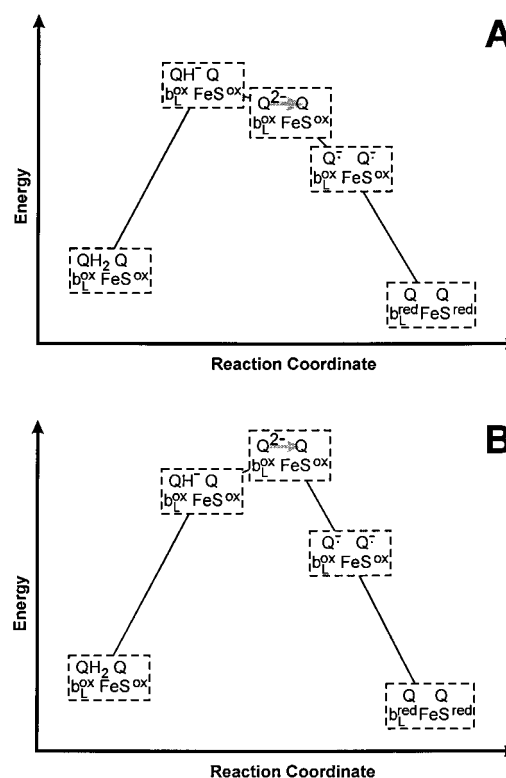


FIGURE 5: Energy Profile of the Center P Reaction. Qualitative illustration of the proposed activation barrier for the oxidation of ubihydroquinone (A) and plastoquinone at center P of the cytochrome *bc*₁ complex according to the proton-gated charge transfer hypothesis. The dashed boxes indicate the approximate energy levels of the reaction intermediates. For simplicity, binding and release of the substrate quinone were omitted. The other quinone is the “prosthetic” quinone, which is not exchanged during normal catalysis. The gray arrow indicates the formation of the charge transfer complex between the two quinone headgroups, promoting the second deprotonation of the hydroquinone. See text for further details. b_L^{ox} and b_L^{red} , oxidized and reduced low-potential heme of cytochrome *b*; FeS^{ox} and FeS^{red} , oxidized and reduced Rieske iron–sulfur cluster; Q, quinone; $Q^{\bullet-}$, semiquinone; QH_2 , QH^- , and Q^{2-} , protonation states of hydroquinone.

stabilization of a charged ubiquinone species at center P would not be desirable as it would disfavor electron transfer onto the iron–sulfur cluster and heme b_L .

Another aspect of this interpretation is that an additional charge in the environment of the bound ubihydroquinone is expected to increase *C* and thereby the activation barrier by electrostatic repulsion. This is perfectly in line with the control of the center P reaction by the redox state of heme b_L as proposed in the proton-gated charge transfer mechanism (Brandt, 1996).

Taken together, our results are best interpreted by assuming a relatively small contribution of *C*, which means that the effective *pK* of the group deprotonating upon formation of the transition state is not very different from the limit values of 14 and 16 estimated for the bovine and yeast enzyme, respectively. We conclude that this group is most likely identical with the substrate ubihydroquinone and that its effective *pK* is not changed very much upon binding to center P. Most of the activation barrier is then interpreted as the energy required to deprotonate ubihydroquinone (Figure 5A). In other words, we propose that the low occupancy of the singly deprotonated ubihydroquinone controls the steady state of the cytochrome *bc*₁ complex.

Mechanism with Plastohydroquinone as a Substrate. When PBH was used as a substrate, steady-state activity was only one-sixth compared to NBH. This marked difference was somewhat unexpected, as the experiments were performed at saturating substrate concentrations and hydrophobicity, midpoint potential, and p*K* values differ only slightly between the two types of quinones (Rich, 1984). The observation that the pH profile was governed by the same p*K* values with both quinones suggested that there was also no fundamental difference in the reaction mechanism, like that plastohydroquinone reacted at a different site.

However, the second pronounced difference between the two substrates provided some clues on their markedly different catalytic competence. While the pH dependence of the activation energy followed an $n = 1$ dependence with NBH, the slope with PBH reflected at least $n = 2$ deprotonations (see Figure 4 and Table 2). Following the same line of arguments discussed above, one would have to conclude that with PBH the transition state would be best described by the doubly deprotonated form of the hydroquinone. Still, no influence of the midpoint potential of the primary electron acceptor, the iron-sulfur cluster, was observed. This could be interpreted such that in the case of PBH both deprotonations of the hydroquinone preceded the first electron transfer (Figure 5B) as proposed by the proton-gated charge transfer mechanism (Brandt, 1996). According to this hypothesis the second deprotonation is facilitated by the formation and symproportionation of a charge transfer complex between two quinone-species bound at center P (cf. Figure 5A). This process is expected to be rather sensitive to the arrangement of the quinone headgroups, which provides a plausible explanation for the appearance of the second deprotonation in the activation barrier, if one simply assumes that this nonphysiological substrate binds in a slightly different orientation. This would prevent proper formation of the charge transfer complex, raising the effective p*K* for the second deprotonation (Figure 5).

While other interpretations might be possible, the proton-gated charge transfer mechanism certainly allows for rationalizing the results presented here in a straightforward way.

ACKNOWLEDGMENT

We thank Franz J. Streb, Williams E. Iyamu, and Steffen Schröder for excellent assistance in performing the experi-

ments. We are indebted to Roy Lancaster, Stefan Kerscher, and Hermann Schägger for careful reading of the manuscript and helpful discussions.

REFERENCES

- Bendall, D. S. (1982) *Biochim. Biophys. Acta* 683, 119–151.
- Brandt, U. (1996) *FEBS Lett.* 387, 1–6.
- Brandt, U., & Trumpower, B. L. (1994) *CRC Crit. Rev. Biochem.* 29, 165–197.
- Brandt, U., Schägger, H., & von Jagow, G. (1988) *Eur. J. Biochem.* 173, 499–506.
- Brandt, U., Haase, U., Schägger, H., & von Jagow, G. (1991) *J. Biol. Chem.* 266, 19958–19964.
- Crofts, A. R., & Wang, Z. (1989) *Photosynth. Res.* 22, 69–87.
- de Vries, S., Albracht, S. P. J., Berden, J. A., & Slater, E. C. (1981) *J. Biol. Chem.* 256, 11996–11998.
- Ding, H., Robertson, D. E., Daldal, F., & Dutton, P. L. (1992) *Biochemistry* 31, 3144–3158.
- Ding, H., Moser, C. C., Robertson, D. E., Tokito, M. K., Daldal, F., & Dutton, P. L. (1995) *Biochemistry* 34, 15979–15996.
- Engel, W. D., Michalski, C., & von Jagow, G. (1983) *Eur. J. Biochem.* 132, 395–402.
- Geier, B. M., Schägger, H., Brandt, U., & von Jagow, G. (1992) *Eur. J. Biochem.* 208, 375–380.
- Giessler, A., Geier, B. M., di Rago, J.-P., Slonimski, P. P., & von Jagow, G. (1994) *Eur. J. Biochem.* 222, 147–154.
- Iwata, S., Saynovits, M., Link, T. A., & Michel, H. (1996) *Structure* 4, 567–579.
- Kagawa, Y., & Racker, E. (1971) *J. Biol. Chem.* 246, 5477–5487.
- Kraicz, P., Haase, U., Gencic, S., Flindt, S., Anke, T., Brandt, U., & von Jagow, G. (1996) *Eur. J. Biochem.* 235, 54–63.
- Kuila, D., & Fee, J. A. (1986) *J. Biol. Chem.* 261, 2768–2771.
- Lancaster, C. R. D., Michel, H., Honig, B., & Gunner, M. R. (1996) *Biophys. J.* 70, 2469–2492.
- Link, T. A. (1994) *Biochim. Biophys. Acta* 1185, 81–84.
- Link, T. A., & von Jagow, G. (1995) *J. Biol. Chem.* 270, 25001–25006.
- Link, T. A., Hagen, W. R., Pierik, A. J., Assmann, C., & von Jagow, G. (1992) *Eur. J. Biochem.* 208, 685–691.
- Marquardt, D. W. (1963) *J. Soc. Ind. Appl. Math.* 11, 431–441.
- Mitchell, P. (1975) *FEBS Lett.* 59, 137–139.
- Prince, R. C., & Dutton, P. L. (1976) *FEBS Lett.* 65, 117–119.
- Rich, P. R. (1984) *Biochim. Biophys. Acta* 768, 53–78.
- Schägger, H., Link, T. A., Engel, W. D., & von Jagow, G. (1986) *Methods Enzymol.* 126, 224–237.
- Trumpower, B. L., & Edwards, C. A. (1979) *J. Biol. Chem.* 254, 8697–8706.
- Wan, Y.-P., Williams, R. H., Folkers, K., Leung, K. H., & Racker, E. (1975) *Biochem. Biophys. Res. Commun.* 63, 11–15.
- Warshel, A. (1979) *Photochem. Photobiol.* 30, 285–290.

BI970968G